Orthopaedics & Traumatology: Surgery & Research 108 (2022) 103372

Contents lists available at ScienceDirect

Orthopaedics & Traumatology: Surgery & Research

journal homepage: www.elsevier.com

Original article

Three-dimensional imaging of the distal radius with reference to volar locking plate surgery

Koichiro Mizuno*, Kotaro Sato, Gaku Takahashi, Yoshikuni Mimata, Kenya Murakami, Minoru Doita

Iwate Medical University, Iwate Ika Daigaku, Japan

INFO ARTICLE

Historique de l'article :
Reçu le 13 février 2022
Accepté le 6 juin 2022

ABSTRACT

Background. – The watershed line is widely accepted as the distal limit of the volar locking plate (VLP); however, the VLP placement could vary depending on the plate contour and morphology of the distal radius. The aim of this study was to investigate the morphology of the distal radius and VLP fitting using 3D images.
Hypothesis. – We hypothesized that attachment of the VLP would affect the contour of the volar prominence of the distal radius.
Patients and methods. – Variable-angle LCP two-column volar distal radius Plate 2.4 and 16 formalin-fixed cadavers were studied. The plate and forearm were scanned using a computed tomography scanner. The plate was fixed to the radial shaft in the most distal position without flexor pollicis longus tendon contact. Postero-antero and lateral radiographs were obtained using fluoroscopy. Postero-antero radiographs were superimposed on a 3D image of the distal radius. The virtual plate was attached to the distal radius in the computer simulations and the plate was adjusted in the sagittal plane. In the postero-antero radiographs, the distance between the plate and distal end of the radius (DPR) was measured. In the sagittal plane, the height of the volar lunate facet (VLF) and the plate-to-bone distance of each locking screw hole was measured. The volar cortical angle (VCA) was measured as the angle formed by a line drawn along the volar surface and a line drawn on the radial shaft on the sagittal plane at each locking screw plane.
Results. – A significant correlation was observed between the height of the VLF and the DPR and between the height of the VLF and the VCA. The plate-to-bone distance at the ulnar screw hole was significantly smaller than that of the other screw holes.
Discussion. – Our study revealed that the higher the VLF, the more proximal is the VLP. The plate fits on the bone surface at the ulnar side, whereas the radial side has more space between the plate and bone.
Level of Evidence. – III, diagnostic Level.

Abbreviations

VLP	volar locking plate
VLF	volar lunate facet
DPR	distance between plate and distal end of the radius
VCA	volar cortical angle
FPL	flexor pollicis longus

1. Introduction

The volar locking plate (VLP) is one of the preferred treatments for patients with unstable distal radius fractures [1–3]. Previous studies have attempted to clarify the morphology of the distal radius with reference to VLP surgery [4,5]. The volar ridge of the distal radius, known as the watershed line, was first described by Orbey et al. [2]. The watershed line is widely accepted as the distal limit of the VLP; however, the VLP placement could vary depending on the plate contour and morphology of the distal radius. Buzzell et al. reported plate and bone contact using a pressure-sensitive film. The average values for plates ranged from 3% to 6%, and all plates made point contact with the bone [6].

* Corresponding author. Department of Orthopaedic Surgery, Iwate Medical University, 2-1-1, Idaidori, Yahaba-cho, Shiwa-gun, Iwate 028-3694, Japan.
Adresse e-mail : kurihara0223@yahoo.co.jp (K. Mizuno).

https://doi.org/10.1016/j.otsr.2022.103372

The volar cortical angle (VCA) was reported as the angle formed by a line drawn along the volar surface of the distal radius and a line drawn on the radial shaft [7–9]. Although a previous report used VCA to investigate plate-to-bone fit, the 3D morphology of the distal radius would contain more complexity. Clinical studies using 3D images provide useful information and computerized anatomical evaluations can be performed accurately with a less invasive 3D investigation [8–13].

The aim of this study was to investigate the morphology of the distal radius and VLP fitting using 3D images. We placed VLPs on the cadaver wrist in the most distal position without flexor pollicis longus (FPL) tendon contact. We hypothesized that attachment of the VLP would affect the contour of the volar prominence of the distal radius.

2. Materials and methods

The ethics committee of our institution approved the study (MH2020-127). We studied variable-angle LCP two-column volar distal radius Plate 2.4 (VALCP; Depuy Synthes, West Chester, PA). This plate is currently widely used and has an anatomically precontoured design. We used extra-small or small plates depending on the fitting to the patients. These sizes are commonly used in Japan. A convenience sample of 16 formalin-fixed left upper limbs (10 males and 6 females; age 72–92 years) without traumatic changes was used. These specimens were donated to our institute for educational and research purposes. The mean width of the distal radius was 30.5 mm (range 27–34). The flexor muscle was exposed by dissection of the skin and subcutaneous tissue on the forearm. We maintained the origin of the FPL muscle in its anatomical position, whereas the pronator quadratus was removed. Prior to plate placement, the forearm and plate were scanned using a 16-row multislice computed tomography scanner (ECLOS; Hitachi Medical Corporation, Tokyo, Japan).

2.1. Plate placement and radiography

All plate fixations were performed by the first author under direct vision. The plates were attached in the most distal position without FPL tendon contact and with the best fit in the radioulnar position according to Kikuchi et al. [14]. The plate was fixed to the radial shaft using a cortical screw. Another orthopedic surgeon confirmed that the plate was not in contact with the FPL tendon with a wrist extension of 30°. Postero-antero (PA) and lateral radiographs were obtained using fluoroscopy.

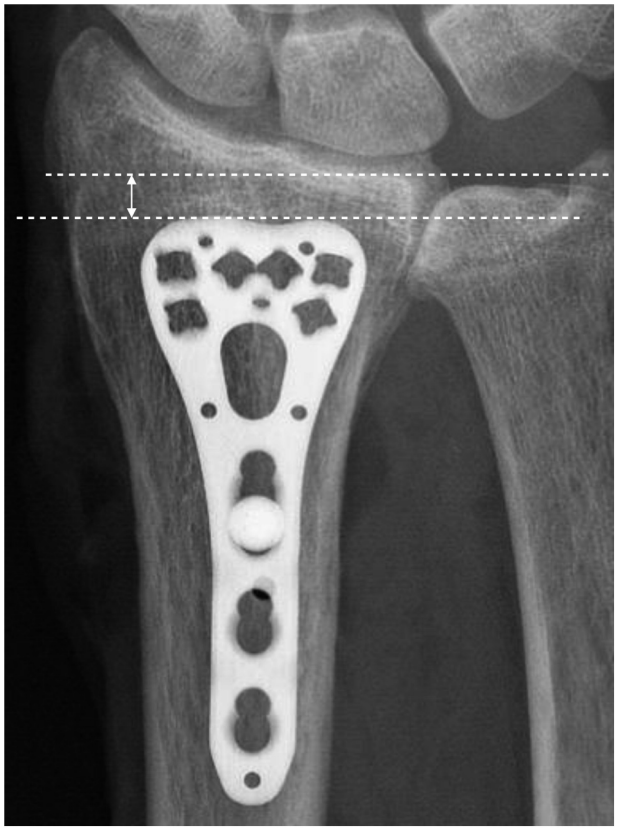

Fig. 1. A line is drawn perpendicular to the radial shaft over the plate end and distal radius. An arrow indicates distance between plate-to-distal end of the radius (DPR).

2.2. Measurement of the PA radiographs

In the PA radiographs, a line was drawn perpendicular to the radial shaft over the plate end and distal radius (Fig. 1). The distance between the lines indicates the distance between the plate and distal end of the radius (DPR). Radiographic parameters were measured using a PACS imaging system (FUJITSU, Tokyo, Japan).

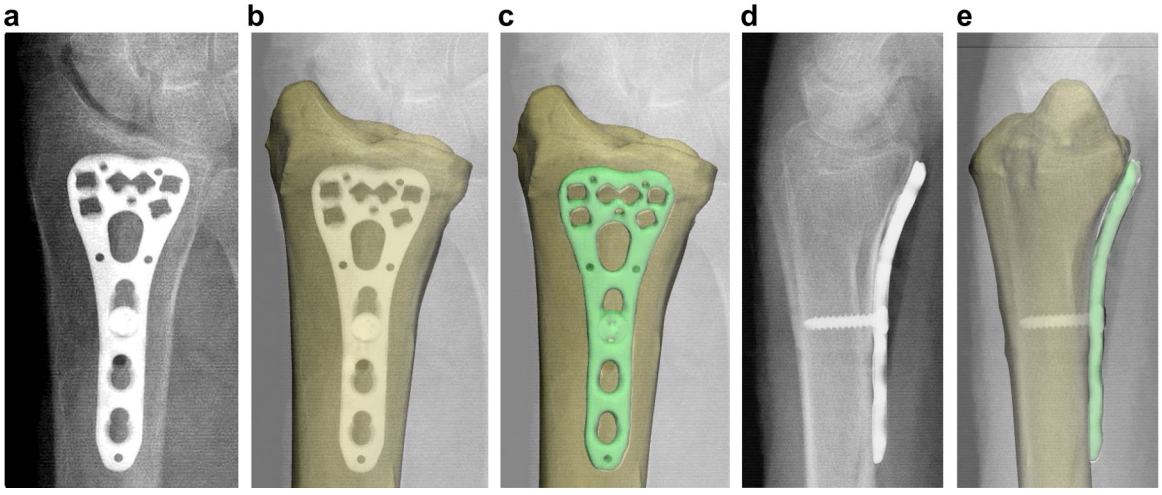

Fig. 2. Plate positioning methods in the computer simulation. A. Postero-antero radiographs. B. 3D bone model is superimposed on postero-antero radiograph. C. 3D plate model is superimposed on the images. D. On the sagittal view, the plate is adjusted without plate-bone intersections. E. Fitting is confirmed in reference to lateral radiographs.

Table 1
Measurement results of the height of the VLF, DPR, VCA, and the plate-to-bone distance.

			Mean	SD
The height of the VLF		(mm)	10	1.5
DPR		(mm)	2.4	1.3
VCA		(mm)		
	H1		28.6	4.3
	H2		30.1	4.8
	H3		35.5	6.2
	H4		41.1	5.7
The plate-to-bone distance		(mm)		
	H1		1.3	0.5
	H2		1.2	0.4
	H3		1.1	0.4
	H4		0.5	0.3

VLF: volar lunate facet; DPR: distance between plate and distal end of the radius; VCA: volar cortical angle.

2.3. Methods for plate positioning in the computer simulation

All imaging data were transferred to a dedicated software program to create 3D images of the forearm and plate (Mimics version 24 and 3-matic version 16; Materialise N.V., Leuven, Belgium). PA radiographs were superimposed on a 3D image of the distal radius (Fig. 2). As a reference, the plate position on the PA radiograph was attached to the distal radius in the computer simulations. On the sagittal plane, the plate was adjusted to obtain an optimal fit without plate-bone intersections.

2.4. Measurement of the 3D images

We marked the apex of the volar lunate facet (VLF) and the flat surface of the distal radius. In the sagittal view, we defined the height from the flat surface to the apex of the volar lunate facet as the height of the VLF (Fig. 3). In the bone and plate images, we defined each locking screw hole in the distal row as H1, H2, H3 and H4 (Fig. 4). We created images of the sagittal section at the center of the screw hole (Fig. 4). In each image of the sagittal section, we measured the distance from the plate to the farthest point of the volar surface. We defined this value as the plate-to-bone distance in H1, H2, H3 and H4 (Fig. 5a). In the same image, the VCA was measured as the angle formed by a line drawn along the volar surface and a line drawn on the radial shaft in H1, H2, H3, and H4 (Fig. 5b). The first author measured all parameters twice and used the mean of the measurements as the final value.

2.5. Outcome setting and statistical analysis

The heights of the VLF, DPR, VCA, and plate-to-bone distances were measured. We examined the correlation between the DPR and the height of the VLF and between the VCA and the height of the VLF. We compared the plate-to-bone distances and the VCA between H1, H2, H3, and H4.

Pearson's test was used for correlations between DPR and the height of the VLF and between VCA and the height of the VLF. One-way analysis of variance with the Tukey test was used to evaluate the plate-to-bone distance between H1, H2, H3, and H4. Statistical significance was set at $p < 0.05$. Data analyses were conducted using Stat Mate 4 software (Tokyo, Japan).

3. Results

The heights of the VLF, DPR, VCA and plate-to-bone distances are shown in Table 1. The VCA at H4 was significantly larger than that at H1 ($p < 0.001$), H2 ($p < 0.001$) and H3 ($p < 0.05$). The plate-to-bone distance at H4 was significantly smaller than that at H1 ($p < 0.001$), H2 ($p < 0.001$) and H3 ($p < 0.01$). A significant correlation was observed between the height of the VLF and DPR ($p < 0.01$, r = 0.67) (Fig. 6) and between the height of the VLF and VCA in H4 ($p = 0.02$, r = 0.56) (Fig. 7).

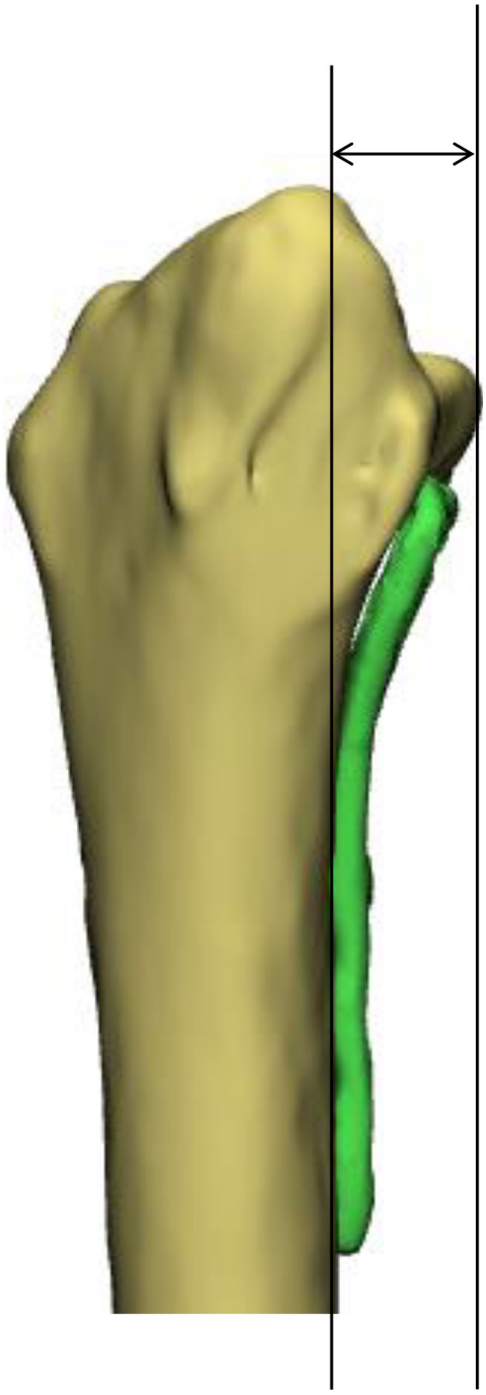

Fig. 3. Methods of measurement in the computer simulation. Height from the cortical screw hole to the apex of the volar lunate facet is defined as the height of the volar lunate facet (VLF).

4. Discussion

In this study, the VCA on the ulnar side was larger than that at the radial side. Evans et al. measured the VCA at the midpoint of the scaphoid fossa, at the lateral edge of the lunate fossa, and at the medial edge of the lunate fossa [15]. They reported that the VCA at

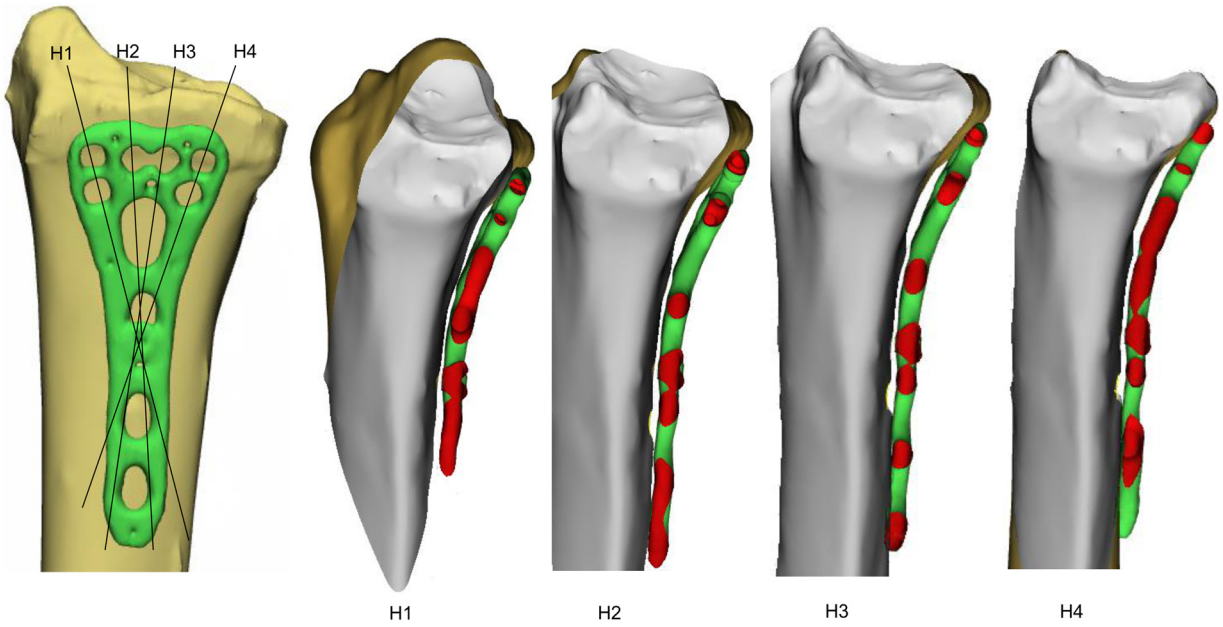

Fig. 4. The locking screw hole of the distal row indicates H1, H2, H3, and H4. Each line indicates the sagittal section in H1, H2, H3, and H4. Figure shows sagittal section of each screw hole.

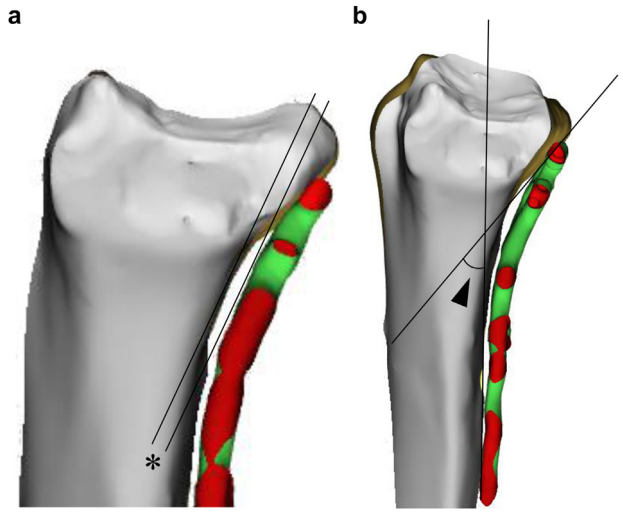

Fig. 5. A. Sagittal section in H4. Asterisk indicates the plate-to-bone distance. B. Sagittal section in H3. Black arrow head indicates volar cortical angle (VCA).

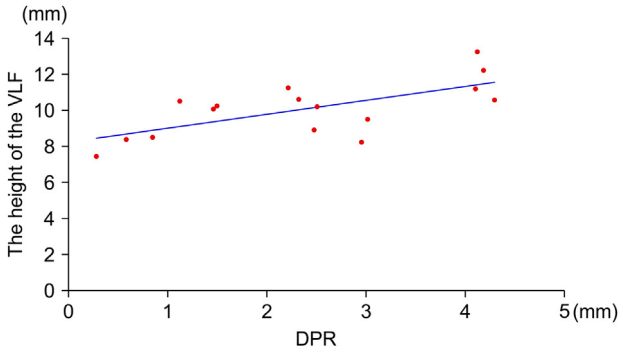

Fig. 6. The height of the VLF was positively correlated with DPR.

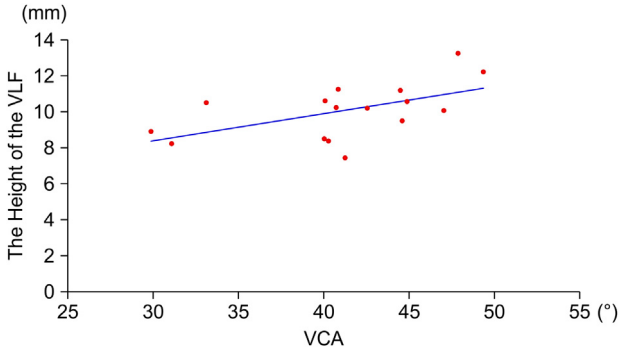

Fig. 7. The height of the VLF was positively correlated with VCA.

the midpoint of the scaphoid fossa was significantly smaller than that at the lunate fossa. Our results are similar to those of Evans et al.

The plate-to-bone distance at H1 was significantly larger than that at H4. This result indicates that the plate fits most of the bone surface at the ulnar side, whereas the radial side has more space between the plate and bone. This result supports previous reports that plates make point contact with the bone [6,16]. Kwak et al. reported the VCA of commercially available VLPs [8]. They reported that the VCA of the VLP used in this study was 21° in the radial column and 27° in the intermedial column [8]. We speculated that the compatibility of the plate would increase if the plate changed its form to lower VCA angles at the radial column. Further studies are necessary to establish a consensus on this issue.

Yoneda et al. studied the plate-to-bone fit using radiographic parameters [16]. They measured the teardrop inclination angle (TIA), which is the angle formed by the volar lunate facet and radial shaft. The study concluded that a low TIA showed better compatibility than a high TIA. The current study revealed that the higher the VLF, the more proximal is the VLP. The height of the VLF affects plate compatibility. In addition, the height of the VLF correlated with VCA. Surgeons can predict whether a plate can be placed distally or proximally from lateral radiographs of the uninjured side. These topics would be useful for treating patients with distal radial fractures. However, further investigations on related factors forming volar ridge, including the type of distal radioulnar

joint, shape of the carpal bone, and deformity due to osteoarthritis, are necessary.

Our data were obtained using a 3D computer model and we did not directly measure the plate-to-bone distance. Gehweier et al. studied the screw length of the VLP using both a 3D printed bone model and a scanned 3D computer model [11]. They reported a high correlation between the two methods and concluded that the computer model was less invasive and reliable. The strength of this study is its 3D simulation using superimposed data. Superimposition with radiographs and 3D images can accurately recreate plate placement in the PA direction. In the sagittal view, the flat surface of both the radial shaft and VLP was advantageous for confirming fitting without plate-bone intersections. This method can evaluate plate and bone relations in detail without image artifacts.

This study has several limitations. First, the sample size was small. Second, the plate was placed without FPL tendon contact. This technique involved subjective decisions and could have affected the VLP placement. To handle this error, two surgeons confirmed VLP placement. Our procedures would be more in line with clinical practice than previous studies that did not consider tendon irritation [8,9,11,16–19]. It would be useful if surgeons can predict the distal setting of VLPs without FPL irritation. Third, we used formalin-fixed cadavers, which may alter soft tissues and muscles. Matityahu et al. studied the contact pressure between the FPL and VLP using fresh-frozen cadavers. In this study, the pressure showed a 7% increase in wrist extension from 25° to 60° [20]. A study using fresh cadavers may increase the reliability of measurements. Fourth, we used Japanese specimens with plates from Western countries. A previous study described that the VCA was larger in Caucasians than in Koreans [21]. The use of specimens from Western countries may have led to different results. Fifth, although we attached the plate with the best fit in the radial-ulnar position, the plate might not be attached accurately. This may have affected the measurements. Finally, we used only a one-plate design. Currently, various plates are used, depending on the fracture pattern [5,13,14,22]. Further studies, including other plate designs, would provide useful information.

5. Conclusion

Our study revealed that the higher the VLF, the more proximal is the VLP. The height of the VLF was correlated with the VCA. The plate fits on the bone surface at the ulnar side, whereas the radial side has more space between the plate and bone. Our data could provide surgeons with anatomical features of the distal radius with reference to volar locking plate surgery.

Disclosure of interest

The authors declare that they have no competing interest.

Sources of funding

None.

Author contribution

Conception and the design of the study: Yoshikuni Mimata, Kenya Murakami, and Minoru Doita.

Acquisition of the data and drafting of the manuscript: Koichiro Mizuno, and Kotaro Sato.

Analysis the data: Gaku Takahashi.

Acknowledgment

The authors wish to thank associate professor Jun Yan from the Department of Anatomy of Iwate Medial University for his technical assistance and Professors Jiro Hitomi for his continuous support of this study.

Références

[1] Chung KC, Watt AJ, Kotsis SV, et al. Treatment of unstable distal radial fractures with the volar locking plating system. J Bone Joint Surg Am 2006;88:2687–94.
[2] Orbay JL, Touhami A. Current concepts in volar fixed-angle fixation of unstable distal radius fractures. Clin Orthop Relat Res 2006;445:58–67.
[3] Vernet P, Gouzou S, Hidalgo Diaz JJ, Facca S, Liverneaux P. Minimally invasive anterior plate osteosynthesis of the distal radius: a 710 case-series. Orthop Traumatol Surg Res 2020;106:1619–25.
[4] Imatani J, Akita K, Yamaguchi K, Yamaguchi K, Shimizu H, Kondou H, et al. An anatomical study of the watershed line on the volar, distal aspect of the radius: implications for plate placement and avoidance of tendon ruptures. J Hand Surg Am 2012;37:1550–4.
[5] Limthongthang R, Bachoura A, Jacoby SM, Osterman AL. Distal radius volar locking plate design and associated vulnerability of the flexor pollicis longus. J Hand Surg Am 2014;39:852–60.
[6] Buzzell JE, Weikert DR, Watson JT, Lee DH. Precontoured fixed-angle volar distal radius plates: a comparison of anatomic fit. J Hand Surg Am 2008;33:1144–52.
[7] Gandhi RA, Hesketh PJ, Bannister ER, Sebro R, Mehta S. Age-related variations in volar cortical angle of the distal radius. Hand (N Y) 2020;15:573–7.
[8] Kwak DS, Lee JY, Im JH, Song HJ, Park D. Do volar locking plates fit the volar cortex of the distal radius? J Hand Surg Eur Vol 2017;42:266–70.
[9] Gasse N, Lepage D, Pem R, Bernard C, Lerais JM, Garbuio P, et al. Anatomical and radiological study applied to distal radius surgery. Surg Radiol Anat 2011;33:485–90.
[10] Shigi A, Oka K, Kuriyama K, Tanaka H, Yoshikawa H, Murase T. Three-dimensional analysis of displacement characteristics of dorsally angulated intra-articular distal radial fractures. J Hand Surg Eur 2020;45:339–47.
[11] Gehweiler D, Teunis T, Varjas V, Kerstan D, Gueorguiev B, Kamer L, et al. Computerized anatomy of the distal radius and its relevance to volar plating, research, and teaching. Clin Anat 2019;32:361–8.
[12] Oura K, Oka K, Kawanishi Y, Sugamoto K, Yoshikawa H, Murase T. Volar morphology of the distal radius in axial planes: a quantitative analysis. J Orthop Res 2015;33:496–503.
[13] Toro-Aguilera Á, Martínez-Galarza P, Camacho-Carrasco P, Caballero M, Segur JM. Comparative study between fixed-angle and polyaxial screws in distal radius fixation with two volar locking plates. Orthop Traumatol Surg Res 2021;107:102801.
[14] Kikuchi Y, Sato K, Mimata Y, Murakami K, Takahashi G, Doita M. Ulnar facet locking screw locations of volar locking plates placed without flexor pollicis longus tendon contact: a cadaver study. Orthop Traumatol Surg Res 2020;106:365–70.
[15] Evans S, Ramasamy AA, Deshmukh SC. Distal volar radial plates: how anatomical are they? Orthop Traumatol Surg Res 2014;100:293–5.
[16] Yoneda H, Iwatsuki K, Hara T, Kurimoto S, Yamamoto M, Hirata H. Interindividual anatomical variations affect the plate-to-bone fit during osteosynthesis of distal radius fractures. J Orthop Res 2016;34:953–60.
[17] Drobetz H, Bryant AL, Pokorny T, Spitaler R, Leixnering M, Jupiter JB. Volar fixed-angle plating of distal radius extension fractures: influence of plate position on secondary loss of reduction A biomechanic study in a cadaveric model. J Hand Surg Am 2006;31:615–22.
[18] Mehling I, Klitscher D, Mehling AP, Nowak TE, Sternstein W, Rpmmens PM, et al. Volar fixed-angle plating of distal radius fractures: screws versus pegs-A biomechanical study in a cadaveric model. J Orthop Trauma 2012;26:395–401.
[19] Dahl WJ, Nassab PF, Burgess KM, Pstak PD, Evans PJ, Seitz WH, et al. Biomechanical properties of fixed-angle volar distal radius plates under dynamic loading. J Hand Surg Am 2012;37:1381–7.
[20] Matityahu AM, Lapalme SN, Seth A, Marmor MT, Buckley JM, Lattanza LL. How placement affects force and contact pressure between a volar plate of the distal radius and the flexor pollicus longus tendon: a biomechanical investigation. J Hand Surg Eur Vol 2013;38:144–50.
[21] Kwon BC, Lee JK, Lee SY, Hwang JY, Seo JH. Morphometric variations in the volar aspect of the distal radius. Clin Orthop Surg 2018;10:462–7.
[22] Fardellas A, Vernet P, Facca S, Liverneaux P. Flexor tendon complications in distal radius fractures treated with volar rim locking plates. Hand Surg Rehabil 2020;39:511–5.